Journal of Cultural Heritage 16 (2015) 134–150

Available online at
ScienceDirect
www.sciencedirect.com

Elsevier Masson France
EM|consulte
www.em-consulte.com/en

Original article

Surface luminescence dating of some Egyptian monuments

Ioannis Liritzis*, Asimina Vafiadou

University of the Aegean, Laboratory of Archaeometry, 1 Demokratias Street, Rhodes 85100, Greece

ARTICLE INFO

Article history:
Received 21 December 2013
Accepted 14 May 2014
Available online 18 June 2014

Keywords:
Egyptian monuments
Luminescence
Dating
Archaeology
Dynasties
Dose rate
Equivalent dose
Quartz
SAR
MAAD
SAAD
Bleaching
Stones

ABSTRACT

Surface luminescence dating to Egyptian monuments of the age range 3000 B C to Hellenistic times has been applied for first time. Monuments include the Giza plateau (Sphinx Temple, Valley Temple, Mykerinus), the Qasr-el-Saqha, the Khasekemui tomb and the Seti I Temple with Osirion at Abydos. Equivalent doses were measured by the single and multiple aliquot additive and regeneration techniques, and dose rates by portable gamma ray probes, and with laboratory counting and dosimetry systems. The resulted ages have confirmed most conventional Dynastic dates, while in some cases, predating was obtained by some hundred of years. The dates are discussed in the light of current archaeological opinions.

1. Introduction

Physical methods for the determination of age of stone structures (monuments, altars, temples, monoliths, buildings, cairns, field walls, mortars etc. [1]) almost always use material associated with the construction period, that may contain ^{14}C datable material rather than material directly from the fabric of the construction. However, in many cases, appropriate organic debris is either not available, or the association with the archaeology is insecure. The direct dating of stone surfaces has been an ongoing subject of research since its first application [2,3], until today, and it is coined surface luminescence dating (SLD).

Sole archaeological dating relies on several grounds such as:

- excavated finds from inside and around a building, and written sources;
- thorough attribution of finds to correct stratigraphic order;
- masonry typology and building technique, as well as, investigation of later repairs;
- use of buildings by later habitants [4].

Though archaeological dating in Egypt relies on written sources, there are instances where the Dynastic chronologies do not satisfy the construction age of some monumental structures. Here, we have applied SLD to a selection of six Egyptian monuments for revisiting their dating in the light of current opinions (Fig. 1).

2. Surface luminescence dating (SLD)

Since 1994, application examples derive from Greece, Peru, and elsewhere covering the period third millennium to Classical and Medieval times [5].

The surface luminescence dating (SLD) works as follows: during the process of the preparation of stone blocks (cutting and carving, or sculpturing) and prior to the setting one upon the other (or construction of a building), the solar radiation (UV and optical spectrum) bleaches the stored geological luminescence in the carved stone surface, down to a depth determined by the depth of penetration of light in that material. This exposure – just minutes required for quartz and feldspar bearing rocks used here i.e. granite and sandstone – erases the luminescence to a zero or a near zero residual value. On construction, shielding of the surface occurs and re-accumulation of (archaeo-) luminescence is initiated due to irradiation from ambient radioactivity and continues till excavation and measurement.

* Corresponding author. Tel.: +30 2 241 099 386.
E-mail addresses: liritzis@rhodes.aegean.gr, ioliritzis@gmail.com (I. Liritzis).

http://dx.doi.org/10.1016/j.culher.2014.05.007
1296-2074/

Fig. 1. Map of Egypt from GoogleEarth. The sites are pined in the map.

In fact, the decay of natural radioactivity viz. uranium, thorium, potassium and rubidium along with cosmic rays, provide as a first approximation a constant irradiation field. The minerals in stonewall are therefore irradiated at a constant rate, and hence, acquire latent luminescence at a constant rate. The latent luminescence is released upon exposure to light, setting the signal to zero or near zero, whence the trapping process begins anew. Events which zero the pre existing geo- or archeo-luminescence are intentional (construction) or accidental (seismic events, destruction, that follows sediment cover) exposure to daylight which provides sufficiently energetic photons to induce zeroing.

In the laboratory, the same process is mimicked. The trapped electrons population can be measured by stimulating the crystal by heat (mostly up to $\sim 400\,^{\circ}C$) or visible [mostly blue or green diodes or infrared (IR)] light. These stimulations lead to release of charges some of which eventually recombine with opposite charges and emit luminescence in either or all of ultraviolet (UV) and visible spectrum. The intensity of this light is proportional to the number of charges recombining and this in turn is proportional to trapped charges. This fact is exploited to convert light units to dose units.

The intensity of the emitted light is proportional to the concentration of trapped charges/electrons and hence, to the radiation dose. The relationship is proportional. The latent luminescence signal increases till a saturation of trapped charges occurs.

Complete eviction of electrons from traps of crystalline minerals is desirable although a residual unbleachable (residual) luminescence component often remains. Quartz and feldspars in monolayer are bleached within minutes of sun exposure, but in rocks, it needs dozen of minutes to zero the signal due to overlying layers. This is because sunlight penetrates the upper nano to micron scale depths easier, resulting in fast total bleaching, and goes further too attenuated according to Beer–Lambert's law and other scattering phenomena more complicated, implying random transport of photons in matter through pathways and cascade effects [6]. The direct optical transition to the conduction band (photoionization) gives rise to the near-exponential dependence of bleaching efficiency on photon energy [7–9]. Theoretical calculations and experimental tests define the penetration depth of solar radiation that comply with experimental data on various rock types (marble, granite) i.e. a complete absorption at around 4–5 mm [6]. However, reservations are made for the penetration as exposure time indicates slow bleaching at greater depths. For calcitic rocks, the bleaching is much slower in the order of hours to several dozens of hours, where a residual luminescence level is reached. The latter serves as the initial level upon which radiation growth builds up [6,8,10–12]. Attenuation factors μ were found 0.52–0.90 mm^{-1} for Penteli and Naxos marble quarries and 0.41–0.52 mm^{-1} for granites ($\pm$ 10%).

Laskaris and Liritzis [6] have produced a generalized approach for the bleaching of luminescence signal as a function of depth for every surface rock (marble, marble schist, granite), promoting the functional behavior of cumulative logarithmic or normal distribution type of error function and attributing to the variable coefficients a physical meaning. The construction of a particular equation unique for each material exposed to sunlight versus depth and exposure time has been tested on various rock types and data sets inhering variable errors, that at the end, offers a new way to surface luminescence dating and authenticity. The residual TL/OSL at top surface layer for $CaCO_3$ of marbles is discernible while for granite and quartz is anticipated near zero. An excellent convergence between predicted and experimentally found paramegers reinforce the new procedure.

For ancient walls made by limestone/marble, the solar penetration can reach depths of 5–10 mm, a useful sampling depth for dating of face wall, provided that sampling is made properly during excavation avoiding exposure to sunlight. Otherwise, sampling from internal contacts between two overlied blocks, solar penetration ensures complete zeroing only in the first 1–3 mm from surface. Incomplete bleaching from variable solar exposure may be determined by applying the dose plateau test. For granites, the complete bleaching of luminescence in top layers of rocks varies

with the attenuation coefficient m and light exposure time, and at any rate, this depth seems to lie between 1 and 5 mm depending from the particular rock opaqueness.

Making use of the TL/OSL drop as a function of exposure time (with the assumption that the rate of trapping due to natural environmental radiation is negligible in comparison to the rate of detrapping due to bleaching), as well as, the Beer–Lambert Law for luminescence drop per depth, and combining these two, a double exponential function is produced giving the Luminescence curves versus depth and exposure time [6].

This light (luminescence) is stimulated by exposure to heat/light: named thermally (TSL or TL)- or optically stimulated luminescence (OSL). The radiation dose since a total charge eviction event when divided by the annual dose rate gives the age i.e.

$$\text{Age} = \text{Total luminescence/annual rate of luminescence acquisition}$$

Given that luminescence is proportional to the dose, the above equation can be rewritten as:

$$\text{Age} = \text{Archaeodose}(D_e)/\text{annual dose}(d_a)$$

where, D_e is the equivalent dose, the laboratory beta dose that induces the same luminescence intensity in the sample as given by a natural (as received) sample, d_a is the annual dose and comprises several components of radiation that arise from the decay of natural radioactive elements i.e alpha, beta and gamma rays of the sample itself and surrounding gamma ray, along with a contribution from the cosmic rays.

Thus, the equivalent dose and the dose rates provide the age of burial of the surface i.e. the construction of the monument.

Based on the above procedures, the timing of the most recent exposure of a stone surface to daylight can be determined. If a carved block in the construction subsequently overlaid this surface, then this approach should provide a direct method for dating the time of construction.

Limestone and marbles (calcite, $CaCO_3$) have been dated using TL [13], and granites, basalt and sandstone has been dated using either OSL (when presence of trace of quartz) or TL, with better results from OSL. Measuring D_e in calcites using OSL has not been successful [14]. Instead, quartz extracted from limestone surfaces has been proposed [11,12,15]. Coring of granites and CCD images have been made [16].

In dealing with dating of ancient buildings and buried sun bleached objects/cobbles, careful sampling and processing is needed and these have been discussed [16–22]. Here, the SLD has been applied to some important Egyptian monuments.

The rationale of this application was three-fold:

- extend the surface luminescence dating method to Egyptian monuments;
- re-assess the credibility of the age of construction compared to surviving inscriptions and historical reports;
- to evaluate errors involved in the methodology arising from the minerals involved and the mixed radiation field of the respective contexts.

3. Archaeological context: samples and sampling

The dated samples derive from the following sites:

1. *Abydos* (Seti A' Temple and Osirion) (RHO-109, Seti I; RHO-110, Seti II; RHO-111 Seti IV; RHO-136, OS3; RHO-137, OS5; RHO-138, OS6; RHO-139, OS7);
2. *Giza: Valley Temple* (RHO-98, VT1; RHO-103, VT6; RHO-105, VT8; RHO-106, VT9a; RHO-107, VT9b);
3. *Giza: Sphinx Temple* (RHO-55, ST1; RHO-56, ST2; RHO-57, ST3; RHO-58, ST4; RHO-59, ST5);
4. *Giza: Osirion Shaft:* (RHO-53, OT1; RHO-54, OT2);
5. Giza: Menkaure's Pyramid: (RHO-119, MYK);
6. *Fayum: Qasr-El Saqa* (RHO-129, QAS1; RHO-130, QAS2; RHO-131, QAS3);
7. *Kings Valley: Khasekhemui Tomb* (Kings Valley) (RHO-132, KH1c; RHO-133, KH2c; RHO-134, KH1) (see, Table 1).

Sampling location described in Table 1 is related to the chronological question of respective monumental complex. These are critically considered in the Discussion section below.

Type of rocks ranged from calcite, basalt, sandstones, granite. The core of the pyramids came from stone quarried in the area already while the limestone, now eroded away, that was used to face the pyramids came from the other side of the Nile River and had to be quarried, ferried across, and cut during the dry season before they could be pulled into place on the pyramid. The Giza plateau however is composed of limestone and sandstone, which is characterised by naturally, eroded cavities. On the other hand, many parts of the bedrock of the plateau were carved to fit individual stones. Certain sections of the pavement were built with a contrasting black basalt. Pink granite, basalt and alabaster were used much more sparingly. Most of this material was moved from various locations in southern Egypt by barges on the Nile. Pink granite probably most often came from the quarries around Aswan as earlier study has shown [11].

Surfaces were detached from walls gently by a hammer and chisel and pieces of inner surface with an area around 2×2 cm. The procedure is made with due caution and by the moment the detached piece becomes loose the external part is covered by a black plastic bag which covers the whole removed piece marking the outer part and with an arrow the inner surface. The sample is unmasked from the plastic bag in the dark room under fume cupboard and red light. Initially, inner surfaces were cleaned by diluted HCl acid to less than 50 μm and powder was removed by gentle rubbing by a small diameter round rasp, because in case of lengthy pointed rasp may sample grains from other adjacent areas with geological origin, to a depth of about 200 μm and less than 1 mm (measured by micrometer) and then sieved to < 40 μm and spread over bronze discs with silicone [23,24]. Fine grain or inclusion was used depending from the availability and amount of grains. Repeatability of luminescence measurements between sub areas of surface was at a level of 20%.

Some characteristic sampling locations are shown in Figs. 2–8 (see more in Supplementary data, Figs. 1–10; also, in http://www.egyptiandawn.info/chapter7.html).

At Giza plateau, the pyramids of Cheops (2528 BC), Chephren (2494 BC) and Mykerinus (2472 BC) dominate the region. The "Osiris Shaft" is the name used to designate a deep burial shaft beneath the Chephren Causeway at Giza (also called "the Water Shaft", or "the Tomb of Osiris Shaft")[26].

Abydos was considered the greatest of all cemeteries and the home of god Osiris. The necropolis area of the city was in use from the earliest times and benefited from royal patronage throughout its history. At Abydos the Temple of Seti I of the 19th dynasty (c. 1306–1290 BC) is the largest, built of fine white limestone and containing splendid relief. Its wall paintings are particularly wonderful, because the colours have been so well preserved, and the quality of the art is of the highest standard. The adjoining building is the Osirion, which features a central "Island of Osiris" made of granitic stone and surrounded by an artificial canal and sandstone wall, all of which were deep underground in pharaonic antiquity, invisible to the eye and unknown to all but the priests.

The temple of Qasr-el-Sagha is at Fayum region (the Land of the Lakes) once near a lake that is now desert. The constructive

Table 1
Luminescence data, monuments, minerals and sampling location, SLD techniques applied per sample and ages. Mineralogical identification was made by XRD.

Sample/location/mineral	SLD technique (SAR, SAAD, by OSL; MAAD by TL)/no. of disc aliquots	Equivalent dose, (Gy)	Annual dose rate (Gy/ky)	Bleaching (hours)/s = sunlight, ss = solar simulator	Temperature (°C)/dose plateau (Gy)	Age (years B C)	Archaeological age estimation (years B C)
1. RHO-53/OT1/Giza Osiris shaft/dacite[a]	Blue OSL, SAAD, 2 discs, inclusion dating	17.55 ± 1.95	3.56 ± 0.16	–	–	2930 ± 600	?
2. RHO-54/OT2/Giza, Osiris Shaft/granite[b]	IR OSL, SAAD, 1 disc, inclusion dating	18.85 ± 2.00	3.87 ± 0.18	3.5 (ss), 5 (s)	–	2870 ± 570	?
3. RHO-98/VT1/Giza, Valley Temple of Chephren's Complex, upper magazine/granite[c]	Blue OSL, SAR, 1 disc, inclusion dating	27.04 ± 2.24	5.34 ± 0.16	–	–	3060 ± 470	4th Dynasty, ca. 2613 to 2494 BC
4. RHO-106/VT9a/Giza, Valley Temple of Chephren's Complex/limestone[d]	MAAD, fine grain	5.12 ± 0.89	1.678 ± 0.068	2, 6, 32 (ss)	310–370	1050 ± 540	4th Dynasty, ca. 2613 to 2494 BC
5. RHO-56/ST2/Giza, Sphinx Temple/limestone[e]	MAAD, fine grain	6.07 ± 0.10	1.44 ± 0.07	1, 2, 3, 5, 7, 10, 20, 40 (s)	340–360	2220 ± 220	4th Dynasty, ca. 2613 to 2494 BC
6. RHO-57/ST3/Giza, Sphinx Temple/granite[f]	IR OSL, SAAD, 2 discs, inclusion dating	20 ± 2	6.27 ± 0.25	5.5 (ss)	–	1190 ± 340	4th Dynasty, ca. 2613 to 2494 BC
7. RHO-58/ST4/Giza, Sphinx Temple/granite[g]	Blue OSL, SAAD, 2 discs, inclusion dating	38 ± 5	8.02 ± 0.22	5 (s), 6.5 (ss)	–	2740 ± 640	4th Dynasty, ca. 2613 to 2494 BC
8. RHO-59/ST5/Giza, Sphinx Temple/granite[h]	IR OSL, SAAD, 2 discs, inclusion dating	41 ± 4	8.03 ± 0.33	5 (ss)	–	3100 ± 540	4th Dynasty, ca. 2613 to 2494 BC
9. RHO-138/OS6/Abydos, Osirion Temple/sandstone[i]	Blue OSL, SAR, 3 disks, inclusion dating	1.96 ± 0.16	0.59 ± 0.08	–	–	1300 ± 570	Middle Kingdom, 11th–14th dynasties, 2134–1690 BC
10. RHO-139/OS7/Abydos, Osirion Temple/granite (black and white grains)[j]	IR OSL, SAR and SAAD, 9 disks, inclusion dating	10.75 ± 1.34	2.70 ± 0.07	5.5 (ss)	–	1980 ± 160	Middle Kingdom, 11^{th}-14^{th} dynasties, 2134-1690 BC
11. RHO-109/SETI I/Abydos, Seti's I Temple/limestone[k]	MAAD, fine grain	4.02 ± 0.35	1.12 ± 0.04	1, 3, 5, 7, 10, 20, 40 (s)	310–320	1580 ± 340	19th Dynasty, ca. 1292 to 1187 BC
12. RHO-110/SETI II/Abydos, Seti's A' Temple/sandstone[l]	MAAD, fine grain	15.6 ± 2.0	2.76 ± 0.17	30 min, 60 min, 140 min, 8 h, 48 h (s)	320–370	3650 ± 800	19th Dynasty, ca. 1292 to 1187 BC
13. RHO-111/SETI IV/Abydos, Seti's A' Temple/sandstone[m]	Blue OSL, SAR, 3 disks, inclusion dating	4.80 ± 0.18	1.35 ± 0.06	–	–	1550 ± 200	19th Dynasty, ca. 1292 to 1187 BC
14. RHO-119/MYK/Mykerinus Pyramid/granite[n]	Blue OSL, SAAD, 1 disk, inclusion dating	41 ± 7	7.52 ± 0.18	–	–	3450 ± 950	4th Dynasty, ca. 2613 to 2494 BC
15. RHO-129/QAS1/Qasr-el-Sagha/limestone[o]	MAAD, fine grain	5.78 ± 0.52	0.86 ± 0.08	13, 24 (s)	340–380	4700 ± 850	Ancient Kingdom to Ptolemaic times
16. RHO-131/QAS3/Qasr-el-Sagha/sandstone[p]	MAAD, fine grain	1.56 ± 0.02	0.93 ± 0.07	1, 2, 4, 6, 10, 20, 40 (s)	240–270	320 ± 128AD	Ancient Kingdom to Ptolemaic times
17. RHO-134/KH1/Abydos, Khasekhemwy/limestone[q]	MAAD, fine grain	5.15 ± 0.24	1.01 ± 0.12	2, 3, 4, 6, 10, 16, 28 (s)	240–270	3100 ± 660	2nd Dynasty, 2890–2686 BC
18. RHO-132/KH1c/ceramic[r]	Blue OSL, SAR, 24 discs, inclusion dating	9.54 ± 0.18	2.27 ± 0.14	–	–	2200 ± 260	2nd Dynasty, 2890–2686 BC

Table 1 (*Continued*)

Sample/location/mineral	SLD technique (SAR, SAAD, by OSL; MAAD by TL)/no. of disc aliquots	Equivalent dose, (Gy)	Annual dose rate (Gy/ky)	Bleaching (hours)/s = sunlight, ss = solar simulator	Temperature (°C)/dose plateau (Gy)	Age (years B C)	Archaeological age estimation (years B C)
19. RHO-133/KH2c/ceramic[s]	Blue OSL, SAR, 22 discs, inclusion dating	9.16 ± 0.04	2.04 ± 0.14	–	–	2490 ± 300	2nd Dynasty, 2890–2686 BC

[a] 2nd sarcophagus, 2nd level. The gamma ray reading was double inside sarcophagus than outside. Height 94 cm, length 246 cm and width 112.5 cm and a lid thickness 20–40 cm. U = 2.51 ppm, Th = 6.9 ppm, K = 1.53%, by PXRF and NAA in NCPR "Demokritos", Athens. Beta dose rate by plastic scintillator was 2.10 ± 0.07.

[b] 3rd sarcophagus, 2nd level, sampling lower part of upper cover. U = 1.4 ppm, Th = 6.6 ppm, K = 2.21% by PXRF and NAA in NCPR "Demokritos".

[c] Inner wall of a blind room surrounded by thick, up to 2 m, granite. There are six such chambers in two rows of three above one another, of very small narrow length and size about 1.80 m high, only a faint hint of sunlight comes down the intact ventilation shaft from the roof. The radioactivity here is highest from all our measurements and taking into account radon emanation it makes these chambers of particular but unknown usage. U = 2.75 ppm, Th = 12.7 ppm, K = 4.11%, by PXRF. Recuperation: 11.55%, Recycling ratio: 0.94.

[d] Inner wall of the roof of the temple, U = 0.8 ppm, Th = 0 ppm, K = 0%, measured by PXRF, and NAA in NCPR "Demokritos". Measurements by TL in limestone following MAAD, which procedure due to the fact that combined optical bleaching (by sun) and TL readings initially was called optical thermoluminecence [25].

[e] Base of the outer wall, in contact with bedrock, in front of the Sphinx U = 2.04 ppm, Th = 1.45 ppm, K = 0% by NAA in NCPR "Demokritos".

[f] Granitic outer wall, in front of the Sphinx, northeast corner of Sphinx temple, on limestone bedrock floor. It was taken from the join between the small granite blocks and the bedrock. U = 2.96 ppm, Th = 20.82 ppm, K = 3.21%, by PXRF, and NAA in NCPR "Demokritos".

[g] Outer wall, lump of granite at the foot of a pillar, in contact with bedrock. U = 2.45 ppm, Th = 45.1 ppm, K = 3.93% by NAA in NCPR "Demokritos". In addition, alpha dose rates by Ge detector was 16.22 Gy/ka and for alpha counting pairs technique 26 ± 1 Gy/ka, the latter obviously influenced by the higher than normal Th activity. The beta dose rates by plastic scintillator was 4.55 ± 0.14 Gy/ka.

[h] Granitic laid into a channel (moat) cut out of bedrock. According to [26], there are two periods of construction for the temple and this granite was laid down on top of it, before the first construction. U = 2 ppm, Th = 10.5 ppm, K = 4.01% by PXRF and NAA in NCPR "Demokritos".

[i] Outer wall of the complex. Grain size 40–80 μm no acid etching, thus, alpha dose rate was accounted for. Regeneration technique by Blue LEDs 20 Gy added dose then 20 preheated combinations of preheatings for 60 s at 220 °C and 0.1 s blue LED readings, and the sequence of 18 readings which followed – no more preheatings – which decayed approximately exponentially. Repeated preheat and read at 0.1 s blue LED for 18 cycles gave unusually constant values with a slight increase, as though preheating is compensating for loss of signal due to bleaching. U = 0.63 ppm, Th = 2.88 ppm, K = 0%, by PXRF. Anomalous fading for TL gives 8 ± 0.6% after 20 days and a sensitivity change 5 ± 5%; the difference of only 3% in the margin of systematic error that implies no fading. On the other hand, by blue OSL and IR results gave 13 ± 1.3% for sensitivity and 8 ± 1.2% for fading that implies no fading; while for IR 11 ± 10 and 71 ± 12, respectively that indicates fading, a difference that is beyond sensitivity correction.

[j] Columns of the temple. U = 2.19 ppm, Th = 8.27 ppm, K = 2.89% by PXRF. Polymineral aliquots of quartz and feldspars. Blue and IR OSL was used.The *k*-value of relative response of beta to alpha was found equal to 0.11 ± 0.0065. It was estimated by additive dose procedure and the ratio of relative responses of betas to alphas. Repeated preheat and read cycles by blue LEDs, that probes both quartz and feldspar, have shown the characteristic ratio for feldspar $1-\mathrm{aln}(n)$, a = 0.276 ± 0.006. It bleaches more slowly than is usual for quartz due to predominance of feldspar. Bleaching with blue LEDs shows that the luminescence falls to 50% after 150 s of continuous exposure, a little slower that the sandstone OS6. IR stimulation with SAAD for repeated cycles of 300 s at 220 °C and 1 s IR exposure approximated the power law, $n-p$, where $p = 0.572 \pm 0.05$, that gives a more constant luminescence for no added dose – the test of good correction. The average D_e based on IR is favored as IR probes only feldspar and blue LED gave variable D_e. The blue OSL and IR did not record any discernible anomalous fading – a signal change before and after 20 days 19% and 17%, respectively was corrected. Sensitivity changes corrected appropriately were 25 ± 1 and 47 ± 0.4 for Blue and IR, respectively. This implies that sensitivity change correction alone accounts fading correction; while for TL noticeable fading was 34% and sensitivity change 5%. The reduction of TL due to solar bleaching for three temperature regions between 280–450 °C, after 30 h a plateau is reached (see Figs. 9–14 in [12]). On the other hand, though not dated, basalt from Giza (80% feldspar mainly anorthite and albite, 15% augite and a little vesuvianite) appeared to have anomalous fading 34 ± 0.1% during 20 days and a sensitivity change 13 ± 0.1%. Murray and Wintle [27] protocol for sensitivity change correction was used for SAR technique applying test dose 10 Gy and regenerated doses up to 40 Gy.

[k] Blind room 2nd floor, contact surface bears plaster. U = 0.91 ppm, Th = 0.23 ppm, K = 0.27% by PXRF, and NAA in NCPR "Demokritos".

[l] Blind room, 1st floor, contact surface bears plaster. U = 0.66 ppm, Th = 3.57 ppm, K = 0.18% by PXRF. Another result from lower blind room northern side, sample no RHO-1075, sandstone, by blue SAR gave ED = 1.08 ± 0.09, annual dose rate 0.35 ± 0.035, and an age 1070 ± 400 years BC, comparable to Seti A' expected age. Another sandstone sample from eastern side of same room gave a geological ED ~ 34 Gy [27].

[m] Roof of the temple, upper corridor, contact surface bearing plaster. Test dose used 10 Gy and regenerated dose up to 40 Gy. U = 1.27 ppm, Th = 5.82 ppm, K = 0.42%, by PXRF. Recuperation: 11.5%, recycling ratio: 0.99

[n] Sample taken from the base of the pyramid. U = 2.26 ppm, Th = 7.43 ppm, K = 3.88% by PXRF and NAA, NCPR "Demokritos".

[o] The second of the seven columns from the left. U = 0.45 ppm, Th = 0.65 ppm, K = 0.06% by PXRF. Ceramic sherds in the building complex cover a long history from Ancient Kingdom to Ptolemaic times even later periods.

[p] Inner room. U = 0.39 ppm, Th = 0.81 ppm, K = 0.14% by PXRF.

[q] Royal cemetery. A piece of wood from the tomb was C-14 dated in Demokritos National Lab, Athens Greece, DEM – 1021 with a calibrated age 2857–2502 BC (based on [28] 95,4%) and at the University of Washington Quaternary Isotope Lab (code no: GX-KH): with a cal C-14 age of 2880–2449 BC (based on [28], 98,4%).

[r] Recuperation: 0.18%, recycling ratio: 1.11.

[s] Recuperation: 1.35%, recycling ratio: 1.05.

material was large sandstone blocks. Unfortunately, the lack of any kind of inscriptions on the temple walls makes difficult an accurate chronological attempt. Nothing is known either for the pharaoh–constructor of the temple or the god it was dedicated to. Ceramic fragments found nearby the vicinity of the temple cover a period of the Old Kingdom to the Early Ptolemaic, Late Roman and Islamic times. Chronological issues of the monuments are discussed in the Discussion section and further archaeological data in e-supplement.

The origin of the building material of several Egyptian monuments have provenance based on petrological analyses (see, statistical groupings in e-supplement).

4. Instrumentation, techniques and measurements

4.1. D_e measurements

Due to the different mineralogical nature of the variety of materials different luminescence techniques were used; in several cases when available amount of grains was adequate, two techniques were applied for comparison purposes (Table 1).

The estimation of D_e can be done using multiple aliquot (MA), single aliquot (SA) or single grain (SG) techniques and in each case, additive dose or regenerative dose procedures are used. In the additive dose procedures, several laboratory doses of varying

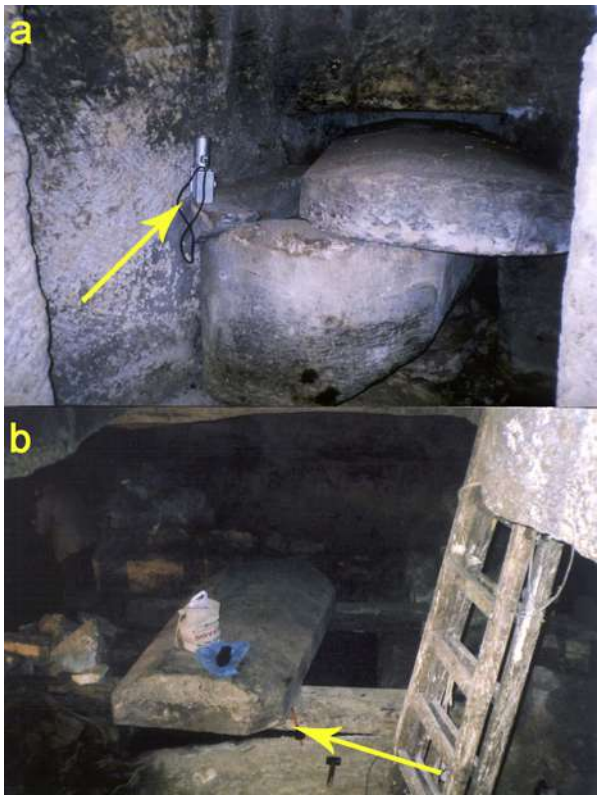

Fig. 2. a: Osirion shaft. View of 2nd sarcophagus, 2nd underground floor beneath the monumental causeway from Chephren to Sphinx. Sampling point of sample no. OT1 (RHO-53); the portable gamma ray reader is shown; b: view of Osirion shaft, 2nd level and 3rd sarcophagus and sampling. Sample no. OT2 (RHO-54).
Photos by IL.

magnitude are given additionally on top of the natural dose of a sample, on several identical sub-samples of a natural sample (so called aliquots). The luminescence signal from the natural dose, as well as the natural plus added doses is plotted against the added doses (zero added dose for the natural) and the relation is fitted with a linear or exponential curve, which describes the growth of the luminescence signal with increasing dose (growth curve). The additive growth curve is extrapolated to the dose axis to provide an estimate of the equivalent dose.

Fig. 3. Inside chamber of blind room where VT1 (RHO-98) was taken from bottom.
Photos by IL.

Fig. 4. The sampling area for sample VT9a (RHO-106) on the roof of Valley Temple of Chefren's complex.
Photo by IL

In the regeneration method, the natural signal is bleached first and then doses are added to construct a luminescence vs dose growth curve. The natural signal is then interpolated on to this regenerated growth curve to estimate the equivalent dose. Amongst the various protocols and techniques used [1], three were used here the multiple aliquot additive dose (MAAD), the single aliquot additive dose (SAAD), and the single aliquot regeneration (SAR). In case of polymineral aliquots of quartz and feldspar, presence IR was used to detect feldspars. It has been concluded earlier [25], that prolonged exposure to infrared could be used to effectively "clean" a quartz sample slightly contaminated with feldspar prior to stimulation by blue light without undesirable influence on the additive dose curve.

A section of characteristic results and plots are shown in Figs. 9–18 (see more in Supplementary data, Figs. 11–22).

In MAAD, each dose point of an additive growth curve is represented by the (mean) thermoluminescence from several aliquots (Figs. 9 and 10). MAAD is suitable for limestone samples and samples for which heterogeneity in zeroing may be excluded (e.g. heating or daylight bleaching at grain level). Further, the geological TL is bleached at various exposure times (Fig. 11). Each residual TL is subtracted from respective additive doses of the build up curve and the dose–temperature plateau test is constructed, whereas the ED is determined from the longer plateau plots (Fig. 10).

For reliable results, it is important to ensure that all aliquots are identical and that the extrapolation is both realistic in terms of the underlying physical mechanisms and accurate. A review of all the normalization procedures to normalize aliquots and evaluate their efficacy to produce identical sub-samples have been

Fig. 5. a: the court of the Sphinx Temple seen from the northeast corner of the roof of the Valley Temple. In the bottom right hand corner, IL is attempting to get a sample, observed by antiquities inspectors. At the far top left may be seen the paws of the Sphinx; b: sample ST4 (RHO-58) from the Sphinx Temple (a). This granite block is below one of the limestone columns (a) in the central hall, inserted into one of the (unknown use) depressions carved into the bedrock at the foot of each column. The sample was taken from the bottom of the granite block where it was pressed tightly against the bedrock; c:view from the sampling location and exact point of sample ST3 (RHO-57); d: ST2 (RHO-56).
Photos by IL.

made [29], as well as, a review on the extrapolation procedures and optimization of the measurement protocols in terms of errors [30]. The advantage of multiple aliquot additive dose (MAAD) is that it averages the luminescence signal over several thousand grains and hence provides a mean age for an ensemble of grains. For heterogeneously zeroed samples, however, non-judicious use of MAAD methods can lead to erroneous results. Almost all samples here by TL of MAAD technique were limestone, except one sandstone (Table 1).

In introducing OSL dating, it has been suggested [31] that it should be possible to make sufficient measurements on a single aliquot to allow a D_e determination. Duller [32] developed a single aliquot method for D_e determination by administering additive doses to potassium feldspar extracts.

This SAAD technique requires correction for sensitivity change during read outs and has been described elsewhere [25,33,34]. In

Fig. 6. The sampling point of sample MYK (RHO-119) in the Mykerinus pyramid.
Photo by IL.

Fig. 7. General view of Osirion temple of sampling location OS7 (RHO-139).
Photo by IL.

Fig. 8. View of Khasekhemwy tomb and his mud made "magazines"; sampling at the rectangular tomb.
Photo by IL.

SAAD, a single aliquot (disc) is measured with consecutively administering beta doses and reading the OSL by short shining from diodes at certain wavelength. The signal growth is fitted by appropriate functions.

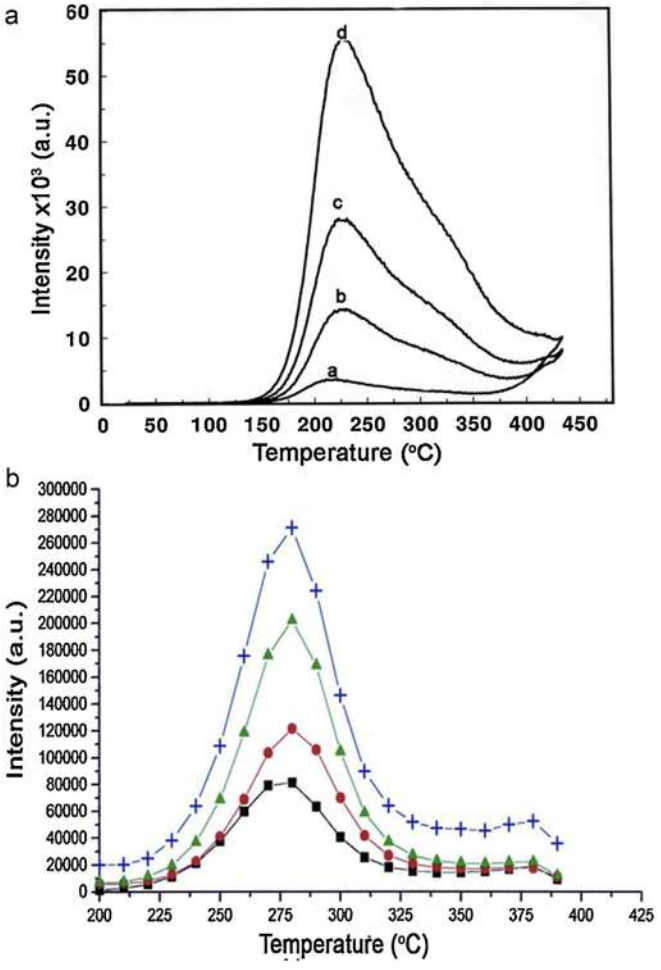

Fig. 9. a: typical TL curves of OS7 (RHO-139), after irradiation with beta doses of (a) 1,2 Gy, (b) 6 Gy, (c) 12 Gy and (d) 24 Gy, with prior preheat at 150 °C for 30 s; b: TL curves of natural and natural + beta dose for VT9a (RHO-106). Lower squares is the average of several natural curves, filled circles natural + 28 Gy, triangles is the natural + 57 Gy and crosses natural + 85 Gy.

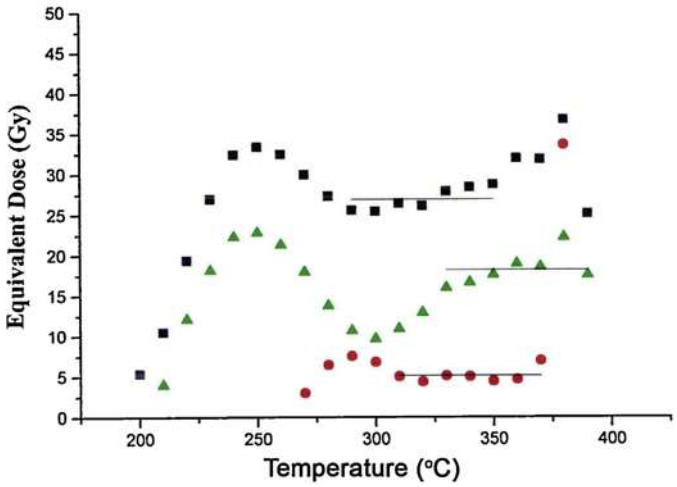

Fig. 10. MAAD technique. Dose–temperature plateau test for valley temple sample VT9a (RHO-106), for bleaching time 2 h (upper squares), 6 h (lower spots) and 32 h (middle triangles). Parallel lines indicate possible plateaux where longer length and smooth is the lower.

The essential information for the correction of SAAD is provided by the decay curve giving the factors, $f(n)$, which is the exponential fit to loss of signal by successive preheats and by which the stable luminescence signal is reduced at the nth preheating and reading of the aliquot and that the $f(n)$ values are essential dose independent. For example, the stimulation of quartz by blue light, the factors $f(n)$ show an exponential dependence:

$$f(n) = e^{-b(n-1)} = r^{(n-1)}$$

where $r = e^{-b} = f(n)/f(n-1)$, that is r is the ratio of any factor to the immediately preceding factor. The correction curve of SAAD by IR due to signal loss of quartz and feldspar followed either the a-relation, 1–aln(n), n is the number of cycles, or the power law p-relation, n^{-p}, n is the number of cycles (Fig. 12).

One consequence of the exponential decay for the correction of single aliquot additive dose measurements is that the correction equations become the same regardless of whether or not the decay of each added component of Luminescence is regarded as being independent of the others.

The correction required is simply:

$$_{corr}L(D_n) = {}_{meas}L(D_n) - r\,{}_{meas}L(D_{n-1}) + {}_{corr}L(D_{n-1})$$

where $_{corr}L(D_n)$ is the corrected value of luminescence resulting from the nth dose D_n and $_{meas}L(D_n)$ is the measured value of luminescence.

The distinction between the first and second correction methods of Duller [32] which was all important for the stimulation of feldspar by infrared disappears for the stimulation of quartz by blue or green light. Further, the decay factors, $f'(n)$ required to correct single aliquot measurements are replaced by r, which can be determined directly from the ratio of any sequential pair of preheating and luminescence readings with no added dose between (although of course better accuracy may come from averaging a sequence of measurements). Thus, unlike the situation with the infrared stimulation of feldspar, the decay factors can be determined directly (without the iterative process described by Galloway [35]) from decay measurements made on the same aliquot after the additive dose measurements.

The SAR method developed for quartz is now widely used for the dating of sediments [27]. The SAR protocol – given dose D_i, preheat, OSL reading (Li), test dose D_t, preheat, measured OSL (T_i), repeated steps – takes into account possible sensitivity changes during the

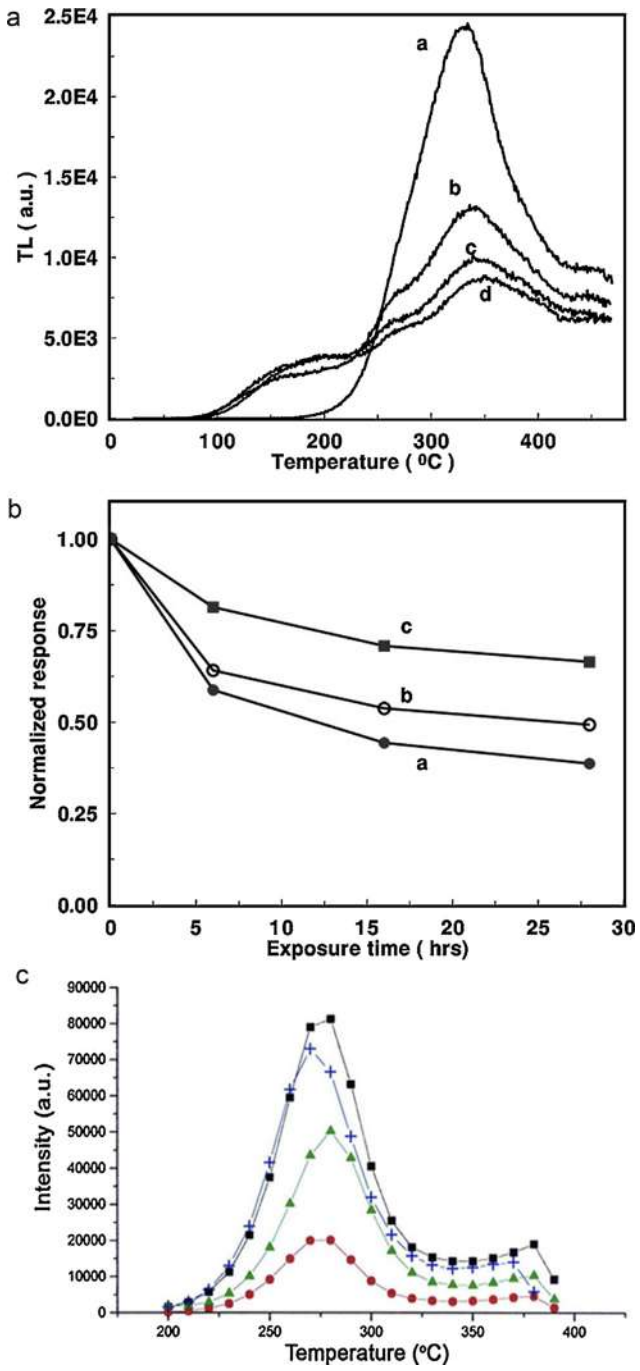

Fig. 11. a: Bleaching of TL of Osirion sample OS7 (RHO-139):(a) geological TL, (b) after 6 h sun exposure, (c) after 16 h and (d) after 28 h sun exposure; b: reduction of luminescence after sun exposure for different temperature regions for sample OS7 (RHO-139) (a) 280–350 °C (b), 360–400 °C and (c) 410–450 °C; c: geological TL Glow curves and bleaching of VT9a (RHO-106). Upper squares is the geological, the lower filled circles after 2 h sun exposure, the crosses is after 6 h and triangles after 32 h.

construction of the regeneration growth curve. Sensitivity may change from repeated irradiation, preheating and OSL stimulation of an aliquot (Fig. 13). When using the SAR or SAAD protocol, several tests and checks are required to ensure reliable D_e values [36–38]. These checks include:

- making sure the sensitivity correction is consistent for identical doses (recycling test);
- testing for any build up of dose from preheating (recuperation test) (see e.g. Fig. 16);
- testing quartz separates for feldspar contamination using IR, and checking anomalous fading tests;
- optimizing the preheat (by plateau tests);
- dose recovery of a known dose;
- plotting D_e against the stimulating time to test for partial bleaching;
- testing samples for sensitivity changes.

If the sample fails any of the test/checks, the data are discarded (Figs. 14 and 15) [18]. The MAAD was used in the absence of quartz, i.e. in calcites with TL (no OSL of calcite is yet possible), and the SAAD and SAR via OSL, when quartz was present. In previous section, the SLD principle was outlined. The inner surface of overlied curved rocks was last exposed to sunlight during construction of masonry. The quick bleaching of quartz and feldspar ensures total bleaching (Fig. 16), while for calcites due to their slow bleaching rate a residual signal might have been remained and define the "zero level". Both cases were checked (see Table 1 notes and below).

We recognize the various sources of error, that are:

- for MAAD scatter arising from differences in the radiation response of different grains of a same mineral inspite of normalization procedure. This may lead to scattering of additive dose points, which to some extent can be compensated by a large number of replicate measurement;
- errors in the measurement of low environmental radiation dose rates, particularly the gamma ray contribution encountered in calcitic contexts of Egyptian sampling sites, where the use of multiple methods was applied, and care was exerted in the counting geometry, accounting also for possible sand/soil cover during the past and that the water content is warranted;
- the destruction of surface datable layer due to friction, weathering and erosion. The development of salts and secondary minerals, and moss/lichens with meticulous examination and handling was possible to remove secondary surface effects. A safe sampling procedure was to divide the inner block surface into several sub areas and this way a geological D_e obviously derived from unidentified drifting (friction) was easily recognized as outlier and excluded [15,39];
- the incomplete bleaching, where if ^{14}C dating is available and shows significantly younger ages, this may point to insufficient bleaching, a situation that would suggests that the rock was not completely bleached, a situation that would result in a bi- or multi-modal distribution of equivalent doses. In our samples, only in one case we had ^{14}C dating made at Khasekhemui tomb, where an excellent agreement was obtained (samples 16–19 of Table 1). At any rate, there can never be a guarantee that stones used to make burial mounds were adequately exposed to light before final burial [23] and hence, notionally the known bleaching per time and depth has to guide sample acquisition from surface.

However, the residual luminescence from incomplete bleaching may be identified from dose–temperature plateau tests for TL [20,23], and for the quartz, feldspar bearing rocks the tests of sensitivity change, anomalous fading, recuperation, pulsed blue LEDs for OSL curves resolving components, comparison of sub areas of a detached inner surface piece [1] are applied. Table 1 gives the data pertaining to each case per each sample, with details at footnotes.

The SAAD is a well-documented technique (though little attention has been drawn) and offers apparent advantages as described here and elsewhere and with some comparison with SAR; the latter is recommended as a thoughtful application.

Details of criteria tests of bleaching, glow curves, additive dose curves, sensitivity change have been performed on all present materials in an earlier work [12]. The concluded remarks are summarized as follows.

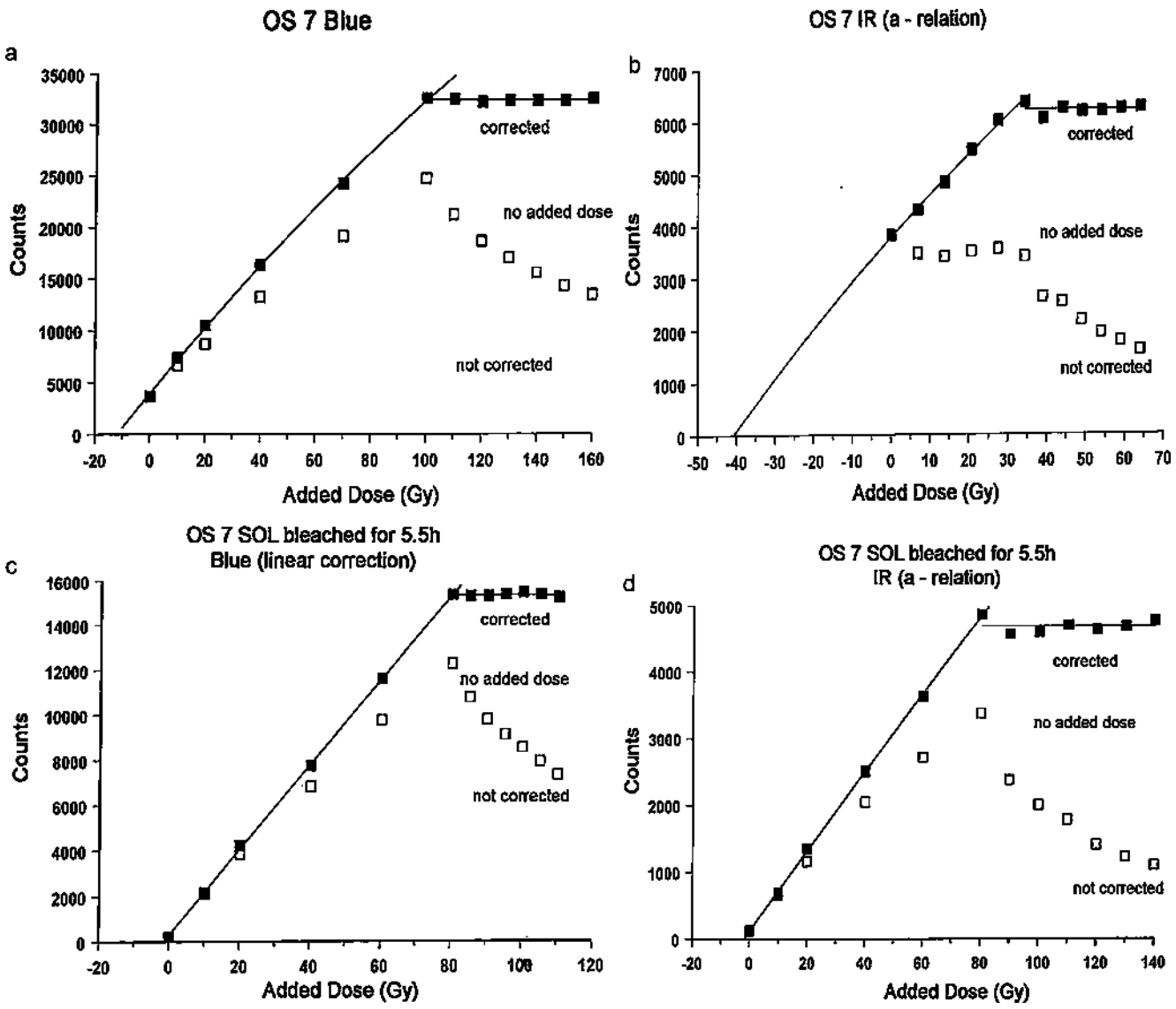

Fig. 12. a: SAAD for D_e calculation for Osirion OS7 (RHO-139) with blue OSL (preheat at 220 °C για 60 s) and reading after short shine of 0.1 s. The D_e deduced from corrected curve (filled squares) equals 12.0 ± 1.5 Gy; b: SAAD for D_e calculation for Osirion OS7 (RHO-139) with IR for 1 s after preheating at 220 °C for 300 s. D_e deduced from corrected curve (black squares) equals 40.8 ± 10.4 Gy (applying *a*-relation); c: SAAD for D_e calculation OS7 (RHO-139), using blue light for 0.1 s (preheating at 220 °C for 60 s) after SOL exposure for 5.5 h. D_e deduced from corrected curve (black squares) equals 1.5 ± 0.3 Gy; d: SAAD for D_e calculation of sample OS7 (RHO-139) by IR for 1 s (preheat at 220 °C for 300 s) after SOL exposure for 5.5 h. D_e deduced from corrected curve (black squares) equals 2.0 ± 0.7 Gy, applying *a*-relation.

The OSL and TL measurements made on present rock types, that is, granites, sandstone which comprise mainly of quartz and feldspar, have proved the potential use of these materials for dating in archaeology (provided that ancient monuments were made of these). This result is based on the well-known quartz and feldspar solar bleaching of sedimentary deposits [12,40,41].

The most rapid bleaching of the Optically Sensitive Electron Traps is observed for sandstone, followed by granite, while for the Thermally Sensitive Electron Traps, the faster bleaching is for granite followed by sandstone and basalt. The granite with quartz, feldspar and biotite (e.g. Mykerinus) bleaches slower than granite with its two-grain phases, mainly feldspar with little quartz and biotite (Osirion) (Fig. 9). The criteria applied for dating purposes, that is, the solar bleaching and the radiation dose growth (either in additive or regeneration mode), are both well satisfied with thermal and optical stimulated luminescence, for three rock types, while the calcites studied follow the known behavior of TL bleaching verifying earlier studies [7,8,33,40]. The solar simulator (SOL) induces luminescence for long durations evidenced from OSL measurements, and the higher preheat seems to affect the D_e, though at present not distinguishable from use of shorter preheat, within the errors. Between the TL and OSL, the latter applied on a single aliquot minerals, except of calcites, offers additional advantages over TL regarding, rapidity, accuracy and effectiveness. Various applied criteria for potential dating included pulsed blue light stimulation, different preheating and solar simulator bleaching, while the single (and multiple) aliquot regeneration and additive dose procedures were used for equivalent dose determination. Some anomalous fading, where noticeable, are included in Table 1.

It has been shown that bleaching with depth, concerning granites and gneisses, reaches the inner geological dose at ~5 mm for corrected IR signal, and that light attenuation is 90% at 3–4 mm depth [9]. This is comparable to the results reported earlier for granites [17,39].

However, the complete bleaching of luminescence in surface layers of rocks varies with the attenuation coefficient μ and light

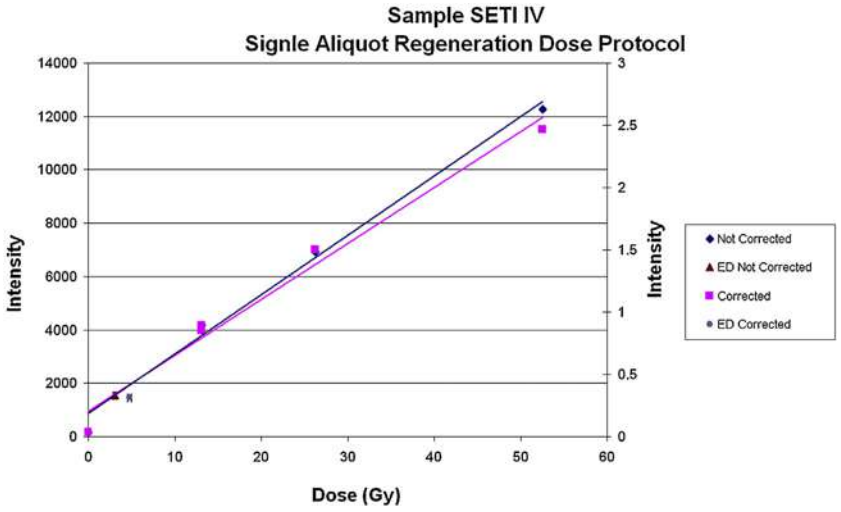

Fig. 13. Typical blue SAR technique for SETI IV (RHO-111). Line with rhombus without correction of test dose Triangle near the origin is natural signal of 3.1 Gy, without correction. Squares are corrected points. Cross point is corrected natural luminescence of 4.80 Gy. Errors are within symbols.

exposure time, and at any rate, this depth seems to lie between 2 to 5 mm depending from the particular rock opaqueness, for granites, quartzites, calcites.

The above examples indicate that the fast (within minutes) solar bleaching of luminescence of quartz grains in monolayer is not applied to solid rocks, due to polymineral phase and to the erosion of the rock surface both making solar radiation intensity attenuate (Fig. 17). Moreover, it is proved that solar radiation bleaches luminescence in rock surfaces, the percentage of signal diminution depends on exposure time, material structure (rock density, mineralogy, defects, pores, cracks), penetration depth, and energy spectrum) [3,6,9,22]. Archaeologists believe that the exposure of such stones to sunlight amounts to at least 2 days, or 25 h of daylight (at least during the period between the two equinoxes) [23].

A generalized approach for every surface rock promoting the functional behavior of cumulative logarithmic/normal distribution type of error function for the bleaching of luminescence signal as a function of depth has been produced [6]. The construction of a particular equation, unique for each material exposed to sunlight versus depth and exposure time, offers a new way to surface luminescence dating. In fact, the distribution of residual TL signal, after bleaching, as a function of depth x, follows the cumulative logarithmic normalized distribution found earlier [6], while attributing to coefficients a physical meaning. An error function fitting provides the best modelling for marbles, granites and sandstones, where absorption coefficient and residual luminescence parameters are defined per each type of rock or marble quarry, that for the latter can get down to 20 mm for long light exposures [18]. The new model has been applied on available data and age determination tests and is considered as a functional behavior that applies to all similar rock types.

Taking into account the above, the total equivalent doses of the different material types (granite, sandstone, limestone) were measured following **MAAD** for samples VT9a (RHO-106), ST2 (RHO-56), SETI I (RHO-109), SETI II (RHO-110), QAS1 (RHO-129), QAS3 (RHO-131), KH1 (RHO-134), the **SAAD** for samples OT1 (RHO-53), OT2 (RHO-54), ST3 (RHO-57), ST4 (RHO-58), ST5 (RHO-59), MYK (RHO-119),, OS7 (RHO-139), and the **SAR** protocol for samples VT1 (VT-98), OS6 (RHO-138), SETI IV (RHO-111), KH1c (RHO-132) and KH2c (RHO-133).

Because this project lasted for long measuring techniques applied were adjusted with the available technique used in the respective laboratory, except if calcite that MAAD with TL was always used, while the availability of grains retrieved from surfaces permitted application more than one technique for comparison purposes.

The MAAD measurements were made on a home made system on the Laboratory of Nuclear and Elementary Particle Physics, of the Physics Department, of the Aristotle University of Thessaloniki, with a Littlemore type 711 reader, equipped with a glow oven evacuated down to 0.1 Torr and high purity N_2 flowing. The light emission was detected by an EMI QA PM tube and glow curves were stored in a PC via a 1024-channel ADC card operating in the MCA mode. The heating strip was nicochrom 0.8 mm thick, with a Cr–Al thermocouple fixed on it. The heating rate was 5 °C/sec, and the irradiator was a $^{90}Sr/^{90}Y$ beta ray source delivering 0.6 Gy/min.

The SAAD measurements were made on the Laboratory of Archaeometry of the University of Edinburgh on a home made instrument equipped with blue, green and IR diodes, which irradiated the disk-sample on a plate [8,42–44]. The disks are heated in a rich N_2 environment at temperatures 50–450 °C with a heating rate 4 °C/s.

The stimulation spectrum is provided by 16 green LEDs type TLMP7513 passing a current of 22 mA per diode and providing approximately 0.2 m·Wcm^{-2} at the sample, with a peak emission at 565 nm (18 nm full width at half maximum). Luminescence was measured by a photomultiplier (PM) EMI type 9635QA preceded by a combination of filters, comprising BG39 (0.5 mm), Schott UG11 (4 mm), Corning 7–59 (4 mm) and 7–60 (4 mm), which give a transmittance peak at 360 nm with transmission exceeding 1% from 330 to 390 nm. The PM noise was about 16 counts s^{-1} and the total background rate about 16 counts s^{-1}, including scattered light. The background rate was measured frequently during the sequences of luminescence measurements and subtracted from them. The light emitting diode and PM combination was mounted on an automatic system, which provided for exposure of the sample to a calibrated beta source, sample heating, and green stimulated luminescence measurement under computer control. The 16 IR LEDs were of type TSUS5402 (Telefunken) with a peak emission at wavelength 950 nm, with intensity that reaches the samples at 50 m Wcm^{-2} and combination of filters BG39 (2 mm), 7–59 (4 mm), giving maximum transmittance at 370 nm with transmission exceeding 1% from 290 to 490 nm. The irradiation of the samples is made by a beta source $^{90}Sr/^{90}Y$ at a rate of 0.1165 Gy/s. Built up curves were of linear, supralinear or saturating response function [24].

The SAR measurements were made on an automated Risø TL/OSL equipped with blue diodes ($\sim$50 mW/cm^2 at 470 $\pm$ 30 nm) and IR laser ($\sim$500 mW/cm^2 at 830 nm) as luminescence simulation

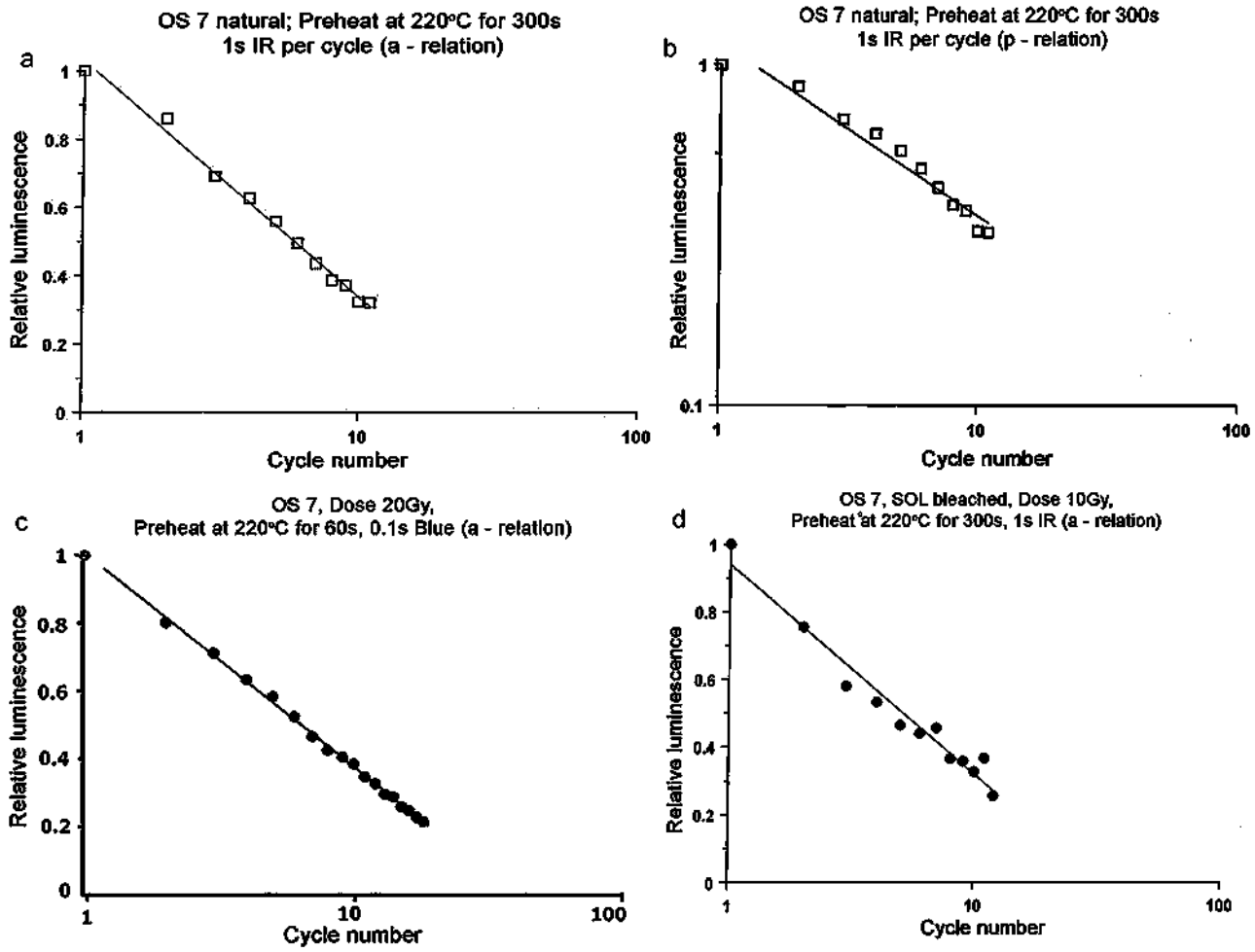

Fig. 14. a: repeat IR measurements relative to the number of cycles for OS7 (RHO-139) on natural signal. In each cycle, preheat at 220 °C for 300 s and IR for 1 s. Corrected curve of the form 1–aln(n), where n the number of cycles and $a = 0.300 \pm 0.008$; b: repeat IR measurements relative to the number of cycles for OS7 (RHO-139). Natural luminescence was used and in each cycle there was a preheat at 220 °C for 300 s and IR reading for 1 s. The corrected curve followed relation n^{-p}, where n the number of repeated measurements and $p = 0.51 \pm 0.14$; c: repeat blue OSL measurements of OS7 (RHO-139) as a function of number of successive measurements. Sample was dosed with 20 Gy. At each cycle, preheat at 220 °C for 60 s and blue reading for 0.1 s. Corrected curve follows relation 1–aln(n), where n the number of repeated readings and $a = 0.276 \pm 0.006$; d: repeat IR measurements OS7 (RHO-139). Sample was bleached in SOL solar simulator and dosed by 10 Gy. In each cycle, preheat at 220 °C for 300 s and then IR for 1 s. Corrected curve follows relation 1–aln(n), where n is the number of repeat cycles and $a = 0.27 \pm 0.02$.

sources. The luminescence is being detected by a 9 mm U-340 filter, and a beta source $^{90}Sr/^{90}Y$ is being attached on the reader. The CETI's reader has a rate of 0.0876 Gy/s and the Danish one 0.024 Gy/s.

For all the three ED approaches, prerequisite is the total bleaching of the luminescence signal. This is most certain with quartz grains (in granitic, sandstone surfaces exposed to sunlight). Avarage values of at least three natural curves for signal and added beta doses from 10–50 Grays were obtained applying normalization to beta dose of 6 Gy and background subtraction.

Regarding the bleaching curves as a function of time and depth, indicative one for the former are given in Fig. 17 and for the bleaching per depth all followed same pattern as published elsewhere for similar rock types [5,11,39]. However, it is shown that bleaching by blue LEDs of granite from Mykerinus pyramid is a little more slowly than sandstone from Osirion OS6. The fast bleaching of the optically sensitive electron traps is 87% within one and half-hours, which is compatible with of bleaching per depth of same sun exposure. However, the large reduction of around 78% occurs in the first 500 s. IR stimulation of dosed (with 200 s beta, approx. 0.25 Gy/sec) single aliquot granite indicates a significant feldspar presence, reconfirming XRD data.

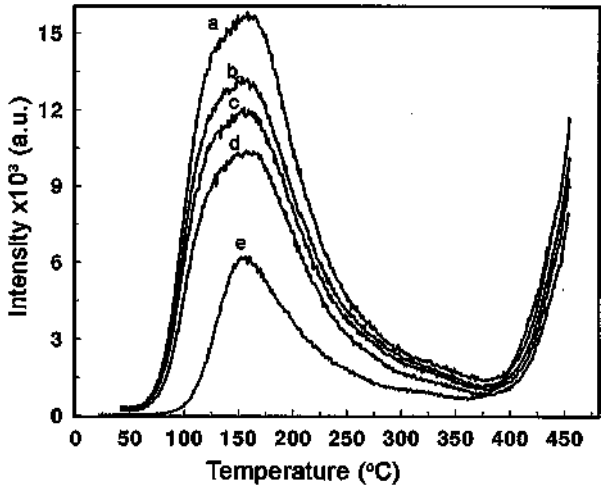

Fig. 15. Typical TL curves of Osirion granite OS7 (RHO-139) after a beta dose of 1.2 Gy. Four repeated measurements (a–d) were taken for the study of sensitivity due to heating. The (e) reading was taken 14 h after irradiation.

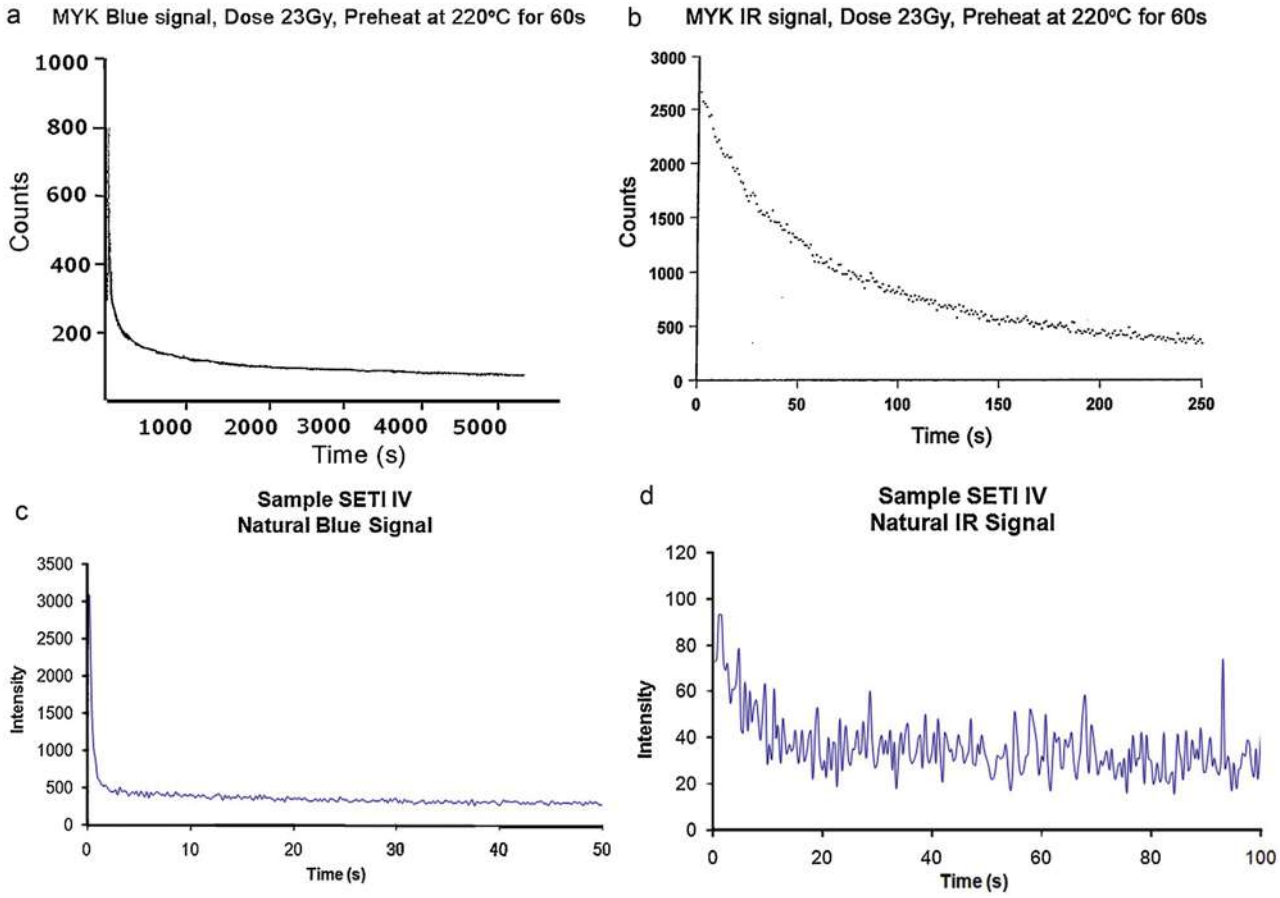

Fig. 16. a: bleaching of Mykerinus (MYK/RHO-119) granite by blue OSL of 23 Gy beta dose and preheat at 220 °C for 60 s; b: bleaching of granite from Mykerinus pyramid (MYK/RHO-119) by IR after irradiation by beta dose of 23 Gy, preheat at 220 °C for 60 s; c: natural luminescence of SETI IV (RHO-111) by blue OSL. Note the fast bleaching of quartz; d: natural luminescence of SETI IV (RHO-111) by IR OSL. Note the poor signal.

Sensitivity changes were monitored and corrections were properly applied (Supplementary data, Fig. 21a). The loss of signal initially is compensated by phototransfer in subsequent repeated cycles.

4.2. Dose rate measurements

The annual dose rates were computed following a combination of techniques; alpha counting pairs technique for the calculation of U and Th. The a-counter used for the specific measurements is the ELSEC Low Level Alpha-Counter 7286 with an EMI 6097B PM tube, and ZnS(Ag) on mylar film, incorporating an internal 6502 microprocessor Case Specific calibration with various standards was made and conversion factors were produced, and also U, Th was calculated by Aitken's formula [45] assuming in both cases, as it is expected, secular equilibrium (unlike in ceramics and soils).

Beta counting measurements were made on a total beta counting system at Riso GM-25-5; with plastic scintillator using a 2″×2″

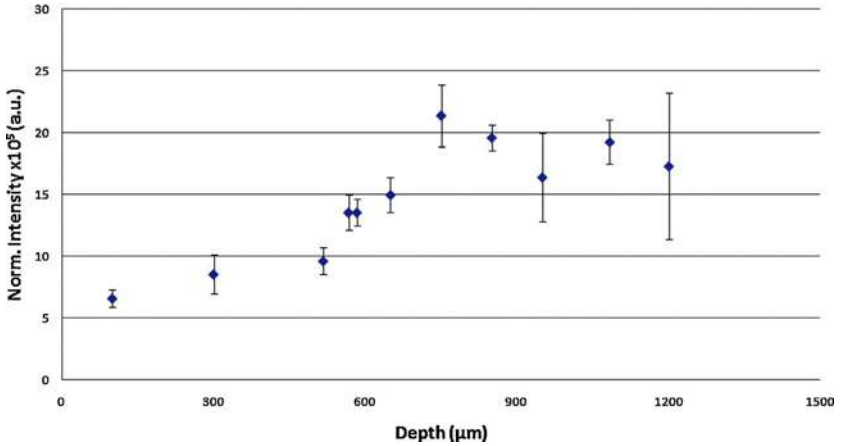

Fig. 17. Bleaching of luminescence as a function of depth below surface for Mykerinus granite (MYK/RHO-119). Surface was exposed to sunlight for 12 h and then eleven layers of ~ 100 μm were removed. Note onset of saturation in about 1 mm.

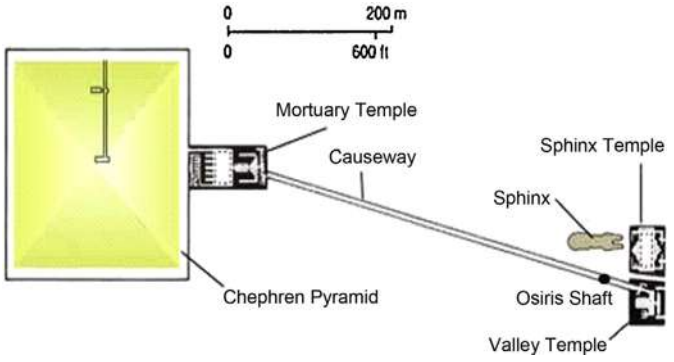

Fig. 18. Overall view of ground plan for the Chephren, the causeway, Osiris shaft, Sphinx Temple and Valley Temple complex.

crystal scintillator NaI(Tl) NE102A and a PM of EMI 9814B, and via a portable XRF TN Spectrace 9000, *s/n* Q-119 for K and Rb values. Hp Ge gamma spectrometry at Edinburgh and at Riso for U, Th, K and to check for U-disequilibrium. Agreement was obtained but for desert sand at Giza and granite ST4 a great discrepancy in U and Th was observed. Neutron activation analysis (NAA) for U, Th (by NCPR Demokritos reactor) was used. All combined methods were compared and values critically assessed. Most discrepant were data by NAA.

Environmental gamma ray dose rates were measured also by a portable scintillometer (spp-2) in counting mode in Gy/ky. The probe was well calibrated inserted at the centre of three radioactive pads, i.e. boxes with high, medium and low radioactivity, as cemented mixture of standard powdered radioactive radioisotopes (at National Center for Physical Research Demokritos, Athens). Values ranged depending from the rock type and counting geometry from 0.10 to 1.2 Gy/ky.

Cosmic ray dose rate was taken as 0.20 Gy/ky but occasionally reduced from attenuation through sand or heavy building material, while sand was 0.20 ± 0.01 Gy/ky. When paste was between two blocks beta dose rate contribution was accounted for (alpha dose rate were stopped at the outer layer of rock surface that was removed by the diluted acid treatment).

The dose rate was occasionally not straightforward due to mixture of radiation fields, the geometry of reading by the portable scintillator, and the fact that they were covered by sand for a considerable period of time. Thus, separate evaluation of radioisotopic content (converted to dose rate) of surrounding rocks was also involved. We present one example at Abydos, sample OS6 (RHO-138) sandstone (same for granite OS7 (RHO-139), to provide a view of the complexity, that was taken into account in each sampling case separately. Here, the gamma ray dose rate from the covered sand was 0.27 mGy/yr (Giza sand). But half of this dose rate of 0.13 mGy/yr was added during the last 1400–1500 years from Coptic period after Roman period (~400–500 AD to 1900 according to information of excavation and historic reports (see for example Edouard Naville's major excavation Report [46]). This gamma dose rate contribution from sand is then 0.13 mGy/year × 1400 years, i.e. 182 mGy/year. During this period, cosmic rays were reduced by sand and the underneath rock blocks, by approx. 20% (of 0.15 mGy/yr cosmic) that makes it 0.03 mGy/yr or finally 0.12 mGy/yr for cosmic, thus, at the end the contribution of environmental radiation was severely altered.

4.3. De determination

Representative measurements and plots are shown in Figs. 9–18 (see more in Supplementary data, Figs. 11–22).

Fig. 9a–c give some characteristic bleaching by blue and IR OSL of Mykerinus pyramid granite (quartz and feldspar) and sandstone in natural state and after dose and preheat. Correction in sensitivity change due to shining and preheating with repeated measurements bleached by blue and IR using *a*- and *p*-relation are shown in Figs. 10a–d. Calculation of ED after correction of sensitivity changes following SAAD by blue or IR light (Fig. 11a–d), additive dose TL curves (Figs. 12a, b), some bleached of TL residual curves after exposure to sunlight (Figs. 13a–c), a typical dose–temperature plateau by MAAD (Fig. 14), and by SAR (Fig. 15), are presented. Several tests were carried out per each sample regarding recuperation, fading, sensitivity change and bleaching per depth from surface (Figs. 17 and 18). Results are similar to those encountered elsewhere in literature.

5. Discussion

The choice of applying luminescence dating to several constructions on the Giza plateau is the intriguing nature and probable (re-) use of them that may mislead construction age. However, current archaeological opinion is that they were built under the auspices of the Fourth dynasty pharaohs Khafre, Khufu and Menkaure. This has been firmly established through the historical record and subsequent discoveries of cartouches at the site. However, the discoveries of cartouches and funerary evidence from earlier dynasties, clearly suggests that parts of the site may have been re-used, and it is a reasonable assumption that some structures were already present at Giza when the large-scale works of the fourth dynasty began.

Today, the traditional theory prevails, that is Giza was built as a funerary complex for the 4th Dynasty pharaohs. However, the lack of contemporary human funerary remains from any Egyptian pyramid and the obvious astronomical and geometric nature of the site, that prove their orientation was not by chance but inhere knowledge and star configuration patterns at the period of construction [47]) imply that the "pyramids as tombs" theory is no longer sufficient and a broader determination of age, function and re-use of both Pyramids and Giza is required. The Old Kingdom monuments are a mystery and conventional dates has been questioned and critically discussed [48].

Table 1 summarizes the dated samples, though in several cases, no satisfactory results were accepted as they did not satisfy tests and criteria applied and thus not included in the table. (examples are given in e-supplement). The drawbacks of some problematic samples, mainly limestone, in brief are referred to e-supplement).

The ages given by the method of luminescence concerns the age of megalithic construction and is the only date that dates these buildings directly and not through archaeological finds and architectural observations. The ages calculated relative to the archaeological age is generally satisfactory, with few exceptions.

The scarcity of acquired powder in some sampling restricted accuracy. Another problem met was the polymineral nature and the use of one single aliquot. In these instances, insufficient bleaching may have occurred.

Regarding the obtained ages compared to archaeological evidence is discussed below (some details on the archaeology of the dated monuments is given in the e-supplement).

The **Sphinx Temple** seems to be dedicated to the Great Sphinx, but we know very little about this, because there is no textural evidence.

A C-14 dating survey, reported in 1999 and more fully in 2001, found on average that the Giza structures were only two centuries older than their conventional dates. The authors of the second survey attributed the older dates to the Egyptian use of "old wood" (or recycled wood) in the charcoal used to make the mortar for the

structures. But the younger sample dates given by the *Cambridge Ancient History* dates, which were about 200 years younger than the 1984 dates, were not explained [49,50].

Radiocarbon dating can only tell us when a tree died, not when it was last used. Wood may lay around for centuries before being burned, especially in a dry climate like Egypt. Thus, the dates on charcoal from the pyramids scatter widely, with many dates older than the historical estimate. The original samples from the Sphinx Temple may have been later intrusions and cannot rule out a pre-Khafra date. But none of the dates for the Sphinx Temple or for Giza as a whole corroborates a prehistoric age [49,51].

The luminescence ages concur with the swayed opinion of a 3rd millennium BC age with an indication of an early 3rd mill. BC and a possible later reuse (intrusion?) during the 13th century BC.

The Valley Temple is next to the Sphinx, which was originally considered as temple related to the Sphinx, but later was recognized as part of the pyramid complex of King Chephren. The buildings of the Valley Temple and the Dead Temple were repaired and modified later by priests operating in the temple during the 5th and 6th dynasty, according to Reisner. Therefore, later finds and repairs may have actually occurred that mislead their construction ages. A verification of these assumptions has been acquired by SLD method. Luminescence ages gave an early 4th mill BC (3000 ± 420 BC) and a New Kingdom one (1050 ± 540 BC, 19th Dynasty).

Along the Chephren Causeway lies the **Osiris shaft** around 35 m below Giza plateau that consists of three carved underground levels with chambers. Because this puzzling causeway runs over other tombs, it is suggested that it may be a later addition. In the 3rd level sampling was taken from an emptied dacitic sarcophagus, as anticipated if it was a symbolic tomb of the God Osiris. No other convincing dating attempt was made. The obtained SLD ages of two sarcophaguses pinpoints to a 4th dynasty age in contradiction to a 16th or early 7th centurt BC, according to archaeological findings inside (Fig. 18). It is still puzzling the difference that may explain an early construction subjected to later reuse activities.

The third group pyramid of Giza located in the southwestern corner of the area attributed to **Mykerinus** (**Menkaure)** by Herodotus and Diodorus the Siculus. It was constructed of limestone and granite. The first sixteen courses of the exterior were made of granite. The upper portion was cased in the normal manner with Tura limestone. The lower part made of granite has smoothed facings, and sampling was made here. The pyramid's date of construction is unknown, because Menkaure's reign has not been accurately defined, but it was probably completed in the 26th century BC. The luminescence age inheres a large error that falls within the early 3rd millennium BC.

At **Abydos**, Khasekem the last king of the 2nd Dynasty changed his name to Khasekhemwy ("the appearance of two powers") apparently after the outcome of political struggle for succession. His tomb at Abydos is a significant departure from the square tomb, in a long and irregular pit, divided into forty warehouses.

The obtaine luminescence age (3100 ± 660 BC) of the rectagular limestone tomb gave a date in agreement to epigraphic and historical evidence (2nd Dynasty, 2890–2686 BC). This result was reinforced also with a calibrated C-14 age of wooden sample from the boats, that provided independent ages from two laboratories ranging 2880–2449 BC (based on [28] 95.4%). Last, two ceramic sherds dated by OSL SAR technique from the re-opened tomb complex provided age span between 2700–2100 BC.

The **Osirion** at the back of the temple of Seti I (1294–1279 BC) is at a lower level and in direct contact with temple. It is a cenotaph and designed to give the impression of an underground mountain or island surrounded by water channels [52]. While there is disagreement as to its true age, despite the fact that it is situated at a lower depth than the structures nearby, that it features a very different architectural approach, and that it is frequently flooded with water which would have made carving it impossible had the water level been the same at the time of construction, Peter Brand says it "can be dated confidently to Seti's reign" [53].

The luminescence ages for **Seti I Temple** gave 1550 ± 200 a concurrent age to archaeological opinion, but one of 3rd mill BC on a sandstone cast doubts. The former is confirmation of textural evidence carved on the sandstone.

Regarding **Osirion**, of the two dates one on sandstone with a large error falls within Seti I reign (1300 ± 500 BC) and the other on granite and low error (1980 ± 160 BC) indicates an earlier by some hundred of years age, and comes from the older part of the temple. The latter implies a somehow earlier construction age of part of Osirion. However, one has to bear in mind that it cannot have been later than about 1800 BC because no building of this kind took place in Egypt between 1800 and 1500 BC due to social collapse. Therefore, the builder had to be from the 12th Dynasty of the Middle Kingdom. There were 12 pharaohs in that time, and the accepted dates of this dynasty were 1976–1793 BC. Egyptian governance and construction did not then recommence until about 1500 BC, i.e. at the New Kingdom. It is known that Seti I carved the sandstone and his reigning dates were 1290–1278 BC [46].

The **Temple at Qasr-el-Sagha** is a small temple and without inscriptions, 8 km north of the lake Birket Qarum, the front end of an horizontal plateau about 34 m above sea level in the northwest of the Fayum [54].

Unfortunately, the lack of any kind of inscription complicates accurate chronology. The only written record with hieroglyphic symbols were nb-tAwy, meaning "King of two places" [55]. Nothing is known about the pharaoh who built the temple or the god to whom it was dedicated. Sherds found near the temple covering a period from the Ancient Kingdom until the Ptolemaic, Roman and Islamic times. Arnold [54] argues that the building dates to the Middle Kingdom. Our dating result does not solve definitely the problem but contributes to that. It indicates an earlier construction re-used probably during much later Ptolemaic times.

Concerning the luminescence measurements, OSL and TL measurements made on particular rock types, that is, granites and sandstone, which comprise mainly of quartz and feldspar, and limestone with or without traces of quartz, has proved the potential use of these materials for dating in archaeology (provided that ancient monuments were made of these). This result is based on the well-known quartz and feldspar solar bleaching of sedimentary deposits. The most rapid bleaching of the optically stimulated electron traps is observed for sandstone, followed by granite, while for the thermal stimulated electron traps the faster bleaching is for granite followed by sandstone. The granite with quartz, feldspar and biotite (e.g. in Mykerinus) bleaches slower than granite with its two-grain phases, mainly feldspar with little quartz and biotite (e.g. in Osirion). These have been quantitatively reported above in dose measurements, from Table 1 and from early work on same materials [12].

The criteria applied for dating purposes, that is, the solar bleaching and the radiation dose growth (either in additive or regeneration mode), are both well satisfied with thermal and optical stimulated luminescence, for three rock types, while the calcites studied follow the known behavior of TL bleaching verifying earlier studies.

The solar simulator (SOL) induces luminescence for long durations evidenced from OSL measurements (thus ED should be corrected for), the higher preheat seems to affect the ED and appropriate corrections are applied based on fitting the additive dose growth curve and fitting the recycling of same aliquot, by exponential functions. Bleaching by SOL must be cautionary as it results often to an induced unbleachable luminescence. The potential dating of ancient monuments made by carved granites, sandstones or limestones, by TL and OSL methods is reconfirmed.

The solar set zero-clock of TL in granites, sandstones and the residual for limestones offers new applications to luminescence of dating ancient megalithic buildings made of these materials.

Between the TL and OSL, the latter applied on single aliquots, except of multiple aliquots for calcites, offers additional advantages over TL, regarding, rapidity, accuracy and effectiveness.

6. Conclusion

Overall, the TL and OSL of sixteen Egyptian monuments were successfully applied with ages that concur with current archaeological opinion though in some cases there was a difference of some hundred of years. The obtained ages dominated between the 1st to 3rd millennia B C with a later exception at Fayum. Dose rates varied too due to different types of materials used. Different calculated and archaeological ages, beyond one standard error, were noticed for one sample at Valley Temple at Chephren's complex (limestone), one at Sphinx Temple (granitic), and one at Seti II Abydos (sandstone).

The mineral properties followed the known behavior but the extracted amount of grains was small which attached a high error to the results, but in more amounts the errors were as anticipated between 5–15%.

The dose rates were under different geometrical setting and mixed radiation fields occasionally were encountered, thus, various methods were employed. A portable gamma reader, as well as, individual radioisotopes per sample measured at the laboratory were used which reconfirmed obtained dose rates, verifying the environmental radiation geometry evaluation of mixed rock types and setting. Comparison between different dose rate techniques identified a couple of discrepancies that were taken into account in the final chosen value. Sand covering some buried settings had to be taken into account.

Blue and IR OSL was used depending from the grain types while the dose plateau was used for pure limestones (and fine grain technique). Sensitivity changes from preheat and/or reading was monitored after repeating readings and correcting build up curves, as well as recuperation and fading.

Acknowledgements

We thank the Supreme Council of Egypt for granting permission to sample and local archaeologists for help during sampling, Dr R.B. Galloway for taking some measurements at Edinburgh and providing some dose rates, Dr. G.S. Polymeris for carrying out some of the TL measurements, Prof. A.S. Murray for allowing AV to carry out some dose rate measurements, Assoc Prof G Kittis, Dr N.Tsirliganis, Dr V. Kilikoglou for allowing AV to carry out some measurements of total dose and dose rates at their premises. AV thanks the State Scholarships Foundation (IKY) for funding the project No. 3450 and Eleni Nakou Foundation, Danish Institute, Rhodes, for a scholarship to Denmark.

Appendix A. Supplementary data

Supplementary data associated with this article can be found, in the online version, at http://dx.doi.org/10.1016/j.culher.2014.05.007.

References

[1] I. Liritzis, A.K. Singhvi, J.K. Feathers, G.A. Wagner, A. Kadereit, N. Zacharias, S.-H. Li, Luminescence Dating in Archaeology, Anthropology and Geoarchaeology: An Overview. SpringerBriefs in Earth System Sciences http://link.springer.com/content/pdf/10.1007/978-3-319-00170-8.pdf
[2] I. Liritzis, Archaeometry: dating the past, EKISTICS 368/369 (1994) 361–366.
[3] I. Liritzis, A new dating method by thermoluminescence of carved megalithic stone building, C. R. Acad. Sci. 319 (ii) (1994) 603–610.
[4] I. Liritzis, The Mystery of Greek pyramidals, Academy of Delphic Studies, Athens, 1998 (in Greek with English summary per chapter).
[5] I. Liritzis, Surface dating by luminescence: an overview, Geochronometria 38 (3) (2011) 292–302.
[6] N. Laskaris, I. Liritzis, A new mathematical approximation of sunlight attenuation in rocks for surface luminescence dating, J. Luminescence 131 (2011) 1874–1884.
[7] I. Liritzis, Y. Bakopoulos, Functional behavior of solar bleached thermoluminescence in calcities, Nucl. Instrum. Methods B 132 (1997) 87–92.
[8] I. Liritzis, F. Foti, P. Guibert, M. Schvoerer, Solar bleaching of thermoluminescence of calcites, Nucl. Instr. Meth. In Phys. Res. B 117 (1996) 260–268.
[9] R. Sohbati, A.S. Murray, M. Jain, Jan-Pieter Buylaert, K.J. Thomsen, Investigating resetting of luminescence signals in rock surfaces, Geochronometria 38 (3) (2011) 249–258.
[10] I. Liritzis, R.B. Galloway, Dating implications from solar bleaching of thermoluminescente of ancient marble, J Radioanal. Nucl. Chem. 241 (2) (1999) 361–368.
[11] I. Liritzis, C. Sideris, A. Vafiadou, J. Mitsis, Mineralogical petrological and radioactivity aspects of some building material from Egyptian Old Kingdom monuments, J. Cult. Herit. 9 (2007) 1–13.
[12] I. Liritzis, G. Kitis, R.B. Galloway, A. Vafiadou, N. Tsirliganis, S.G. Polymeris, Probing luminescence dating of archaeologically significant carved rock types, Med. Archaeol. Arch. 8 (1) (2008) 61–79.
[13] I. Liritzis, Searching for precision of a new "luminescence clock" in dating calcitic rocks, J. Radioanalytical and Nucl. Chem. 247 (3) (2001) 727–730.
[14] R.B. Galloway, Does limestone show useful optically stimulated luminescence? Ancient TL 20 (1) (2002) 1–5.
[15] I. Liritzis, A. Drivaliari, G. Polymeris, C. Katagas, New quartz technique for OSL dating of limestones, Med. Archaeol. Arch. 10 (1) (2010) 81–87.
[16] S. Greilich, U. Glasmacher, G. Wagner, Optical dating of granitic stone surfaces, Archaeometry 47 (3) (2005) 645–665.
[17] J. Habermann, T. Schilles, R. Kalchgruber, G.A. Wagner, Steps towards surface dating using luminescence, Radiat. Meas. 32 (5–6) (2000) 847–851.
[18] A. Vafiadou, M.S. Murray, I. Liritzis, Optically stimulated luminescence (OSL) dating investigations of rock and underlying soil from three case studies, J Archaeol. Sci. 34 (10) (2007) 1659–1669.
[19] I. Liritzis, A. Vafiadou, Dating of megalithic masonry, in: Internat Conference, The Archaeology of World Megalithic Cultures. Rhodes 28–31 Oct 2004, Proceedings in Mediterranean Archaeology & Archaeometry 5 (1) (2005) 25–38.
[20] I. Liritzis, Strofilas (Andros Island, Greece): new evidence of cycladic final Neolithic dated by novel luminescence and Obsidian Hydration methods, J. Archaeol. Sci. 37 (2010) 1367–1377.
[21] I. Liritzis, N. Laskaris, Fifty years of obsidian hydration dating in archaeology, J. Non-Crystalline Solids 357 (2011) 211–219.
[22] R. Sohbati, A.S. Murray, J.P. Buylaert, N.A.C. Almeida, P.P. Cunha, Optically stimulated luminescence (OSL) dating of quartzite cobbles from the Tapada do Montinho archaeological site (east-central Portugal), Boreas 41 (2012) 452–462.
[23] I. Liritzis, P. Guibert, F. Foti, M. Schvoerer, The Temple of Apollo (Delfi) strengthens novel thermoluminescence dating method, Geoarchaeology Int. 12 (1997) 479–496.
[24] D.W. Zimmerman, Luminescence dating using fine grains from pottery, Archaeometry 13 (1) (1971) 29–56.
[25] I. Liritzis, R.B. Galloway, D.G. Hong, Single aliquot dating of ceramics by green light stimulation of luminescence from quartz, Nucl. Inst. Methods Phys. Res. B 132 (1997) 457–467.
[26] H. Ricke, Der Harmachistempel des Chephren in Giseh, Beitraege zur Aegyptischen Bauforschung und Altertumskunde, 10, 1970 (Wiesbaden).
[27] A.S. Murray, A.G. Wintle, Luminescence dating of quartz using an improved single aliquot regenerative dose protocol, Radiat. Meas. 32 (2000) 57–73.
[28] M. Stuiver, P.J. Reimer, Extended ^{14}C Data Base and Revised Calib 3.0 ^{14}C Age Calibration Program, Radiocarbon 35 (1) (1993) 215–230.
[29] M. Jain, L. Boetter-Jensen, A.K. Singhvi, Dose evaluation using multiple aliquot quartz OSL: test of methods and a new protocol for improved accuracy and precision, Radiation Measurement 37 (2003) 67–80.
[30] C. Felix, A.K. Singhvi, Study of non-linear luminescence-dose growth curves for the estimation of paleodose in luminescence dating: results of Monte Carlo simulations, Radiat Meas 27 (1997) 599.
[31] D.J. Huntley, D.I. Godfrey-Smith, M.L.W. Thewalt, Optical dating of sediments, Nature 313 (1985) 105–107.
[32] G.A.T. Duller, Equivalent dose determination using single aliquots, Nucl. Tracks. Radiat. Meas. 18 (1991) 371–378.
[33] I. Liritzis, R.B. Galloway, D. Katsonopoulou, D. Soters, In search of ancient Helike, Golf of Corinth, Greece Journal of Coastal Research, vol. 17 (1) (2001) 118–123.
[34] I. Liritzis, R.B. Galloway, D. Hong, N. Kyparissi-Apostolika, OSL dating of three prehistoric ceramics from Theopetra cave, Greece: a case study. Mediterranean Archaeology & Archaeometry 2 (2) (2002) 35–43.
[35] R.B. Galloway, Equivalent dose determination using only one sample: Alternative analysis of data obtained from infrared stimulation of feldspars, Radiation Measurements 26 (1) (1996) 103–106.
[36] A.G. Wintle, A.S. Murray, A review of quartz optically stimulated luminescence characteristics and their relevance in single aliquot regeneration dating protocols, Radiation Measurements 41 (2006) 369–391.
[37] A.K. Singhvi, M.A.J. Williams, S.N. Rajaguru, V.N. Misra, S. Chawla, S. Stokes, N. Chauhan, T. Francis, R.K. Ganjoo, G.S. Humphreys, A ~200 ka record of climatic

change and dune activity in the Thar Desert, India Quat Sci Rev 29 (23–24) (2010) 3095–3105.
[38] A.K. Singhvi, S.C. Stokes, N. Chauhan, Changes in natural OSL sensitivity during single aliquot regeneration procedure and their implications for equivalent dose determination, Geochronometria 38 (2011) 231–241.
[39] I. Liritzis, N. Zacharias, S.G. Polymeris, Surface luminescence dating of 'Dragon Houses' and Armena Gate at Styra (Euboea, Greece), Med. Archaeol. Arch. 10 (3) (2010) 65–81.
[40] I. Liritzis, Advances in thermo- and opto-luminescence dating of environmental materials (sedimentary deposits): part I: techniques, GLOBAL-NEST 2 (1) (2000) 3–27 (part II: applications. GLOBAL-NEST, vol.2, No. 1, 29-49).
[41] R.G. Roberts, Luminescence dating in archaeology: from origins to optical, Radiat. Meas. 27 (1997) 819–892.
[42] R.B. Galloway, Towards the use of green light emitting diodes for the optically stimulated luminescence dating of quartz and feldspar, Meas. Sci. Technol. 3 (1992) 330–335.
[43] R.B. Galloway, On the stimulation of luminescence with green light emitting diodes, Radiat. Meas. 23 (1994) 547–550.
[44] R.B. Galloway, Comparison of the green- and infrared-stimulated luminescence of feldspar, Radiat. Meas. 23 (1994) 617–620.
[45] M.J. Aitken, Thermoluminescence Dating, Academic Press, London, 1985.
[46] (a) E. Naville, Abydos, J. Egyptian Archaeol. 1 Part1 (1914) 2–8 (Egypt Exploration Fund, London);
(b) E. Naville, Excavations at Abydos: The Great pool and the tomb of Osiris, J. Egyptian Archaeol. 1 (1994) 158–167 (Part 2, Egypt Exploration Fund, London);
(c) E. Naville, The Excavations at Abydos, in: W.M.F. Petrie (Ed.), Under "Egypt Exploration Fund", Ancient Egypt, 1, British School of Archaeology in Egypt, London, 1994, pp. 103–105, 3 pp.
[47] G. Magli, Architecture, in: astronomy and sacred landscape in ancient Egypt, Cambridge University Press, Cambridge, 2013.
[48] R. Temple, Egyptian dawn, Century Press, London, 2010.
[49] G. Bonani, H. Haas, Z. Hawass, M. Lehner, S. Nakhla, J. Nolan, R. Wenke, W. Wolfli, Radiocarbon dates of Old and Middle Kingdom Monuments in Egypt, Radiocarbon 43 (3) (2001) 1297–1320.
[50] M. Lehner, How Old are the Pyramids? Ancient Egypt Research Associates, 2005.
[51] R. Wenke, J. Nolan, A. Amran, Dating the pyramids Archaeology 52 (5) (1999) 26–33.
[52] R. David, A guide to religious ritual at Abydos, Warminster, 1981.
[53] P.J. Brand, The Monuments of Seti I: Epigraphic, in: Historical and Art Historical Analysis, Brill, 2000.
[54] D. Arnold, Fajjum, LÄ 2, 1977.
[55] D. Arnold, Do Der Tempel Qasr-el-Sagha, Mainz, 1979.